Soil Dynamics and Earthquake Engineering ▮ (▮▮▮▮) ▮▮▮–▮▮▮

Contents lists available at ScienceDirect

Soil Dynamics and Earthquake Engineering

journal homepage: www.elsevier.com/locate/soildyn

An alternative approach for the Istanbul earthquake early warning system

Hakan Alcik [a], Oguz Ozel [b,*], Yih-Min Wu [c], Nurcan M. Ozel [a], Mustafa Erdik [a]

[a] Earthquake Engineering Department, Kandilli Observatory and Earthquake Research Institute, Bogazici University, Istanbul, Turkey
[b] Geophysics Department, Engineering Faculty, Istanbul University, Istanbul, Turkey
[c] Department of Geosciences, National Taiwan University, Taipei, Taiwan

ARTICLE INFO

Article history:
Received 11 September 2009
Received in revised form
11 March 2010
Accepted 14 March 2010

Keywords:
Earthquake early warning
Average period
Peak displacement
Magnitude

ABSTRACT

Two recent catastrophic earthquakes that struck the Marmara Region on 17 August 1999 (M_w=7.4) and 12 November 1999 (M_w=7.2) caused major concern about future earthquake occurrences in Istanbul and the Marmara Region. As a result of the preparations for an expected earthquake may occur around Istanbul region, an earthquake early warning system has been established in 2002 with a simple and robust algorithm, based on the exceedance of specified thresholds of time domain amplitudes and the cumulative absolute velocity (CAV) levels (Erdik et al., 2003 [1]). In order to improve the capability of Istanbul earthquake early warning system (IEEWS) for giving early warning of a damaging earthquake in the Marmara Region, we explored an alternative approach with the use of a period parameter (τ_c) and a high-pass filtered vertical displacement amplitude parameter (*Pd*) from the initial 3 s of the P waveforms as proposed by Kanamori (2005) [2] and Wu and Kanamori (2005) [3,4]. The empirical relationships both between τ_c and moment magnitude (M_w), and between *Pd* and peak ground velocity (PGV) for the Marmara Region are presented. These relationships can be used to detect a damaging earthquake within seconds after the arrival of P waves, and can provide on-site warning in the Marmara Region.

1. Introduction

Present technological advances in seismic instrumentation, in digital communication and in computer technologies enable the implementation of real-time earthquake monitoring systems. Effective early warning systems for natural hazards are now increasingly perceived as an integral component of disaster risk reduction programmes. For this viewpoint, earthquake early warning (EEW) is becoming a practical tool to reduce the losses caused by a damaging earthquake by giving a few seconds to a few tens of seconds warning before the arrival of a damaging ground motion [5,6].

EEW systems, already in operation in several countries around the world, have been using mainly two approaches; regional warning and on-site warning. In the first approach, the traditional seismological method is used to locate an earthquake, and determine the magnitude from stations at close epicentral distances, and estimate the ground motion at other distant sites. This approach has already been used in Japan [7], Mexico [8] and Taiwan [9]. In the second approach, the beginning of the ground motion (mainly P waves) observed at a site is used to predict the ensuing ground motion (mainly by S- and surface waves) at the same site. On-site warning is usually based on individual sensors, while regional warning requires seismic networks. Therefore the regional warning approach is more reliable but requires more time, and cannot be used for the sites at short distances, as is the case for Istanbul. In contrast, the second one is less reliable, but it is very fast and could provide early warning to sites even at very short distances, where an early warning is most necessary. In the second approach, it is necessary to make rapid estimation of the nature of the progressing earthquake or the ground motions at an early stage of its rupture process [2].

In this paper, we explore the use of the second approach, namely τ_c and *Pd* methods [2–4,10,11] for seismic early warning purposes in the Marmara Region using the accelerograms from the strong motion networks operated by three agencies: the Bogazici University Kandilli Observatory and Earthquake Research Institute (BU-KOERI), Istanbul Technical University (ITU) and the Ministry of Public Works and Resettlement-Earthquake Research Institute (ERI). Fig. 1 shows the stations distribution of the networks in the northwestern part of Turkey and the events used in this study.

2. Istanbul earthquake rapid response and early warning system (IERREWS)

Frequent occurrence of historic destructive earthquakes clearly demonstrates the high potential of producing a damaging earthquake and also the high potential of seismic hazard in the

* Corresponding author.
E-mail address: oguzozel@istanbul.edu.tr (O. Ozel).

0267-7261/$ - see front matter © 2010 Elsevier Ltd. All rights reserved.
doi:10.1016/j.soildyn.2010.03.007

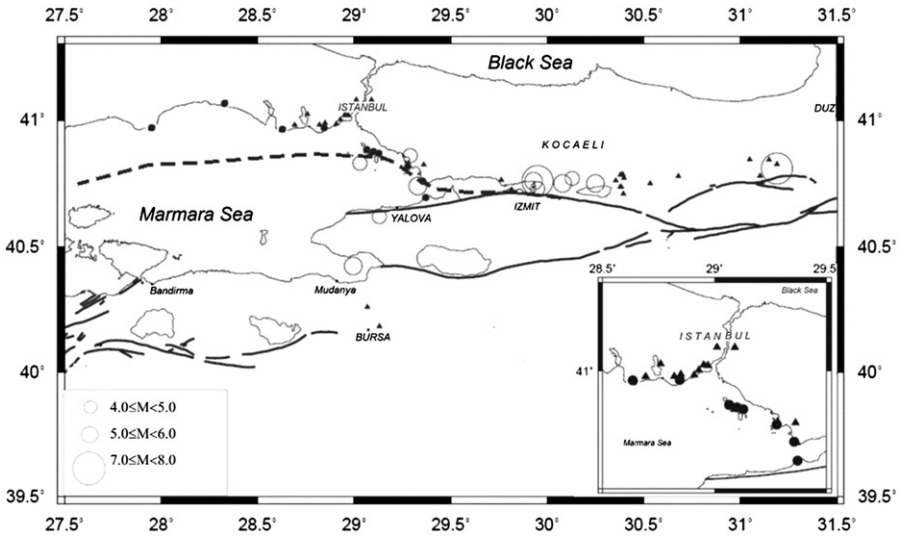

Fig. 1. Epicenter distribution of the earthquakes (open circles) used in this study. Black triangles and filled circles show the strong ground motion stations and IEEW stations, respectively. Inset shows the stations in the down town of Istanbul. Also shown by solid and dashed lines are the branches of the North Anatolian Fault Zone.

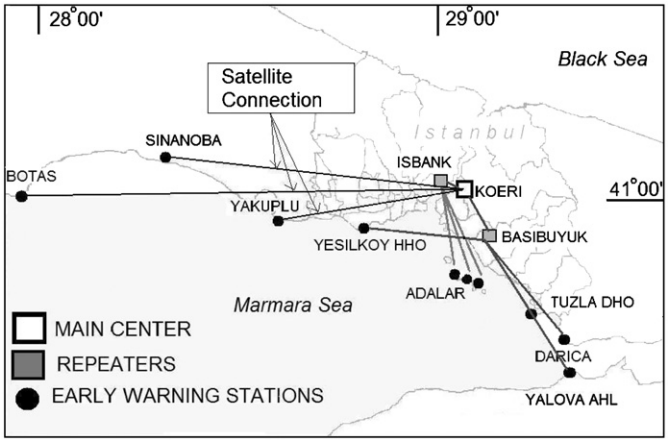

Fig. 2. Distribution of early warning stations and 2.4 GHz spread-spectrum radio modem transmission through repeater stations (filled rectangles). Far stations, BOTAS, SINANOBA and YAKUPLU have satellite links.

Marmara Region. The Izmit (Kocaeli) earthquake of 17 August 1999 (M_w 7.4) and the Duzce earthquake of 12 November 1999 (M_w 7.2), occurred along the western part of the North Anatolian Fault Zone, have caused major concern about future earthquake occurrences and their possible consequences, particularly in the Istanbul area. Current probabilistic estimate of a major earthquake in Istanbul is about 2% per annum [12]. As part of the preparations for the future earthquake in Istanbul, an earthquake rapid response (IERRS) and an early warning system (IEEWS) in the metropolitan area have been implemented in 2002, shortly abbreviated as IERREWS [1]. One hundred (100) of the strong motion instruments are stationed in dense settlements in the Metropolitan area of Istanbul in dial-up mode for rapid response information generation. Ten (10) of the strong-motion stations are installed at locations as close to the Great Marmara Fault as possible in on-line data transmission mode to enable EEW (Fig. 2). Considering the complexity of fault rupture and the short fault distances involved, a simple and robust early warning algorithm, based on the exceedance of specified threshold time domain amplitude levels is implemented. The band-pass filtered peak ground acceleration (PGA) and CAV (the time integral of the absolute acceleration over the duration of the earthquake record) are compared with specified threshold levels. When any PGA and/or CAV on any channel, in a given station, exceeds specific threshold values (currently set at 0.05, 0.1 and 0.2 m/s^2 for PGA and 0.2, 0.4 and 0.7 m/s for CAV [13]) it is considered a vote. Whenever we have votes from at least three stations for the respective threshold value within a selectable time interval (5 or 10 s), the respective alarm level is declared. The early warning information, consisting of one out of three alarm levels, will be communicated to the appropriate servo shut-down systems of the recipient facilities, which will automatically decide proper action based on the alarm level. Depending on the location of the earthquake (initiation of fault rupture) and the recipient facility the warning times for Istanbul can be up to about 8–10 s [1].

3. τ_c and *Pd* methods

For an earthquake early warning system, it is important to estimate the size of an earthquake. Wu and Kanamori [3] developed a method to estimate the magnitude of an earthquake from the first few seconds of strong motion records, by extending the method of Nakamura [14] and Allen and Kanamori [15]. In this method, the τ_c parameter, which characterizes the average period of ground motion during the initial t_0 second after the arrival of the P wave is calculated by using vertical component records to estimate earthquake magnitude, although the value of magnitude is not directly used for on-site early warning purposes. A high-pass filter is applied to remove the drift of the displacement records after double integration of the accelerograms [16]. Since the relationship involving these parameters depends on the specific filter used, it is important to use the same filter consistently [11]. For a complete presentation of the methods, see also Refs. [2,10]. The calculation of τ_c is given by the following equation:

$$\tau_c = 2\pi / \sqrt{[\int_0^{t_0} \dot{u}^2(t)\,dt]/[\int_0^{t_0} u^2(t)\,dt]} \quad (1)$$

where τ_c is in seconds, u is the high-pass filtered displacement of the vertical component ground motion, and $\dot{u}$ is the velocity differentiated from the displacement u.

Another element of EEW is to estimate the strength of shaking at a site from the first few seconds of the P wave. Wu and Kanamori [3] showed that the *Pd* parameter, which is the

Please cite this article as: Alcik H, et al. An alternative approach for the Istanbul earthquake early warning system. Soil Dyn Earthquake Eng (2010), doi:10.1016/j.soildyn.2010.03.007

Table 1
Earthquakes and their parameters of the events used in this study.

Date and time	M_w	Depth (km)	Lat. (N)	Long. (E)	Number of stations[a]
1999 0817 000138[b]	7.5	17	40.760	29.950	9
1999 0820 092855[b]	4.6	10	40.620	29.130	5
1999 0831 081049[b]	5.6	4	40.760	29.930	6
1999 0831 083323[b]	4.7	6	40.730	29.950	5
1999 0913 115527[b]	5.9	10	40.750	30.080	15
1999 0917 195005[b]	4.5	10	40.770	30.130	6
1999 0929 001306[b]	5.0	12	40.740	29.330	8
1999 1020 230820[b]	4.8	7	40.830	29.030	10
1999 1111 144123[b]	5.7	7	40.750	30.250	5
1999 1112 165719[b]	7.2	10	40.810	31.190	1
2000 0707 001530[b]	4.6	10	40.860	29.290	5
2006 1024 140021[c]	5.1	14	40.424	28.995	40

[a] One station corresponds to one vertical component.
[b] BU-KOERI, ITU and ERI database.
[c] Istanbul Earthquake Early Warning and Rapid Response System database.

maximum displacement amplitude can be used to estimate the PGV, and proposed that if *Pd* is equal or greater than 0.5 cm, the event is most likely damaging. Thus, the magnitude and shaking intensity can be estimated for early warning purposes within 3 s after the P wave arrival is detected. If $\tau_c > 1$ s and $Pd > 0.5$ cm, then the potential of a damaging earthquake is quite high [10,17]. They also demonstrated that the combination of the τ_c and *Pd* methods can provide reliable threshold warnings within 10 s after the occurrence of a large earthquake [3,4], depending on the stations density of the seismic network.

4. Data and analysis

The τ_c and *Pd* methods have been studied to determine linear relations for the Marmara Region between τ_c and M_w, and between *Pd* and PGV parameters [10,17]. We used a combined dataset including the events with magnitudes 4.5 and larger, recorded by

Table 2
Information related to the stations and the instruments used in data collection.

Station			Sampling rate	
Code	Lat. (N)	Long. (E)	(samples/s)	Instrument & sensor
E02[a]	40.8178	29.2784	50	GeoSIG, GSR-24, CMG-5T, ±2g
E04[a]	40.9699	28.8445	50	GeoSIG, GSR-24, CMG-5T, ±2g
E07[a]	40.6954	29.3707	50	GeoSIG, GSR-24, CMG-5T, ±2g
R00[a]	40.9805	28.8622	200	GeoSIG, GSR-18, CMG-5T, ±2g
R02[a]	40.9967	28.9051	200	GeoSIG, GSR-18, CMG-5T, ±2g
R09[a]	40.9881	29.0529	200	GeoSIG, GSR-18, CMG-5T, ±2g
R11[a]	40.9851	29.1158	200	GeoSIG, GSR-18, CMG-5T, ±2g
R12[a]	40.8247	29.3249	200	GeoSIG, GSR-18, CMG-5T, ±2g
R13[a]	41.0146	29.0284	200	GeoSIG, GSR-18, CMG-5T, ±2g
R14[a]	41.0063	28.9003	200	GeoSIG, GSR-18, CMG-5T, ±2g
R19[a]	41.0376	28.9443	200	GeoSIG, GSR-18, CMG-5T, ±2g
R20[a]	41.0260	29.0336	200	GeoSIG, GSR-18, CMG-5T, ±2g
R22[a]	41.0148	28.9793	200	GeoSIG, GSR-18, CMG-5T, ±2g
R23[a]	41.0050	28.9694	200	GeoSIG, GSR-18, CMG-5T, ±2g
R25[a]	40.9257	29.1371	200	GeoSIG, GSR-18, CMG-5T, ±2g
R26[a]	41.0314	28.9365	200	GeoSIG, GSR-18, CMG-5T, ±2g
R28[a]	40.8941	29.2416	200	GeoSIG, GSR-18, CMG-5T, ±2g
R29[a]	40.8784	29.2709	200	GeoSIG, GSR-18, CMG-5T, ±2g
R31[a]	40.8659	29.2852	200	GeoSIG, GSR-18, CMG-5T, ±2g
R32[a]	40.8983	29.1740	200	GeoSIG, GSR-18, CMG-5T, ±2g
R36[a]	40.9784	29.1494	200	GeoSIG, GSR-18, CMG-5T, ±2g
R41[a]	41.0113	28.8887	200	GeoSIG, GSR-18, CMG-5T, ±2g
R44[a]	40.8576	29.2941	200	GeoSIG, GSR-18, CMG-5T, ±2g
R48[a]	40.9165	29.2226	200	GeoSIG, GSR-18, CMG-5T, ±2g
R51[a]	40.8344	29.3055	200	GeoSIG, GSR-18, CMG-5T, ±2g
R53[a]	40.9751	29.0451	200	GeoSIG, GSR-18, CMG-5T, ±2g
R55[a]	40.9036	29.1661	200	GeoSIG, GSR-18, CMG-5T, ±2g
R58[a]	41.0042	29.0828	200	GeoSIG, GSR-18, CMG-5T, ±2g
R59[a]	40.8614	29.3225	200	GeoSIG, GSR-18, CMG-5T, ±2g
R69[a]	40.9382	29.1445	200	GeoSIG, GSR-18, CMG-5T, ±2g
R70[a]	41.0183	29.0469	200	GeoSIG, GSR-18, CMG-5T, ±2g
R72[a]	41.0059	29.0479	200	GeoSIG, GSR-18, CMG-5T, ±2g
R75[a]	41.0277	29.0917	200	GeoSIG, GSR-18, CMG-5T, ±2g
R76[a]	40.9191	29.1524	200	GeoSIG, GSR-18, CMG-5T, ±2g
R77[a]	40.9754	29.0948	200	GeoSIG, GSR-18, CMG-5T, ±2g
R80[a]	40.9263	29.1652	200	GeoSIG, GSR-18, CMG-5T, ±2g
R85[a]	40.9898	28.8448	200	GeoSIG, GSR-18, CMG-5T, ±2g
R90[a]	40.9963	28.9181	200	GeoSIG, GSR-18, CMG-5T, ±2g
R92[a]	41.0148	29.1526	200	GeoSIG, GSR-18, CMG-5T, ±2g
R93[a]	41.0133	29.1186	200	GeoSIG, GSR-18, CMG-5T, ±2g
R95[a]	40.9897	29.0742	200	GeoSIG, GSR-18, CMG-5T, ±2g
R97[a]	41.0339	28.9823	200	GeoSIG, GSR-18, CMG-5T, ±2g
409[b]	40.7624	30.3545	200	Kinemetrics, SSA-12, ±0.5g
410[b]	40.7097	30.3953	200	Kinemetrics, SSA-12, ±0.5g
411[b]	40.7863	30.3907	200	Kinemetrics, SSA-12, ±0.5g
412[b]	40.7787	30.6785	200	Kinemetrics, SSA-12, ±0.5g
414[b]	40.7496	30.5326	200	Kinemetrics, SSA-12, ±0.5g
415[b]	40.7369	30.3787	200	Kinemetrics, SSA-12, ±0.5g

Please cite this article as: Alcik H, et al. An alternative approach for the Istanbul earthquake early warning system. Soil Dyn Earthquake Eng (2010), doi:10.1016/j.soildyn.2010.03.007

Table 2 (*continued*)

Station			Sampling rate	
Code	Lat. (N)	Long. (E)	(samples/s)	Instrument & sensor
417[b]	40.7732	30.3978	200	Kinemetrics, SSA-12, ±0.5g
ARC[b]	40.8236	29.3607	200	GeoSys&Terra, GSR-16, SSA-320, ±2g
ATK[b]	40.9890	28.8490	200	Kinemetrics, SSA-12, ±1g
ATS[b]	40.9809	28.6926	200	GeoSys&Terra, GSR-16, SSA-320, ±2g
BRS[c]	40.1830	29.1310	100	Kinemetrics, SMA-1
BUR[b]	40.2605	29.0680	200	GeoSys&Terra, GSR-16, SSA-320, ±2g
CNA[b]	41.0238	28.7594	200	GeoSys&Terra, GSR-16, SSA-320, ±2g
DAR[b]	40.7569	29.3673	200	GeoSys&Terra, GSR-16, SSA-320, ±2g
DHM[b]	40.9823	28.8200	200	GeoSys&Terra, GSR-16, SSA-320, ±2g
FAT[b]	41.0197	28.9500	200	GeoSys&Terra, GSR-16, SSA-320, ±2g
GBR[b]	41.0194	28.9695	200	GeoSys&Terra, GSR-16, SSA-320, ±2g
GEN[b]	40.7849	30.3923	200	GeoSys&Terra, GSR-12, SSA-320, ±2g
GLC[b]	40.7260	29.8150	200	Kinemetrics, SSA-12, ±1g
HAS[b]	40.8688	29.0875	200	GeoSys&Terra, GSR-16, SSA-320, ±2g
HIL[b]	40.6473	29.2645	200	Kinemetrics, SSA-12, ±0.5g
HOS[b]	40.8688	29.0875	200	Kinemetrics, SSA-12, ±0.5g
IST[b]	41.0800	29.0900	100	Kinemetrics, SMA-1
KMP[b]	41.0032	28.9285	200	GeoSys&Terra, GSR-12, SSA-320, ±2g
RUZ[b]	40.6474	29.2768	200	Kinemetrics, SSA-12, ±0.5g
SEK[b]	40.7847	30.3798	200	GeoSys&Terra, GSR-12, SSA-320, ±2g
SKR[b]	40.7370	30.3840	100	Kinemetrics, SMA-1
YKP[b]	41.0811	29.0112	200	GeoSys&Terra, GSR-16, SSA-320, ±2g
YPT[b]	40.7639	29.7620	200	GeoSys&Terra, GSR-16, SSA-320, ±2g
ZYT[b]	40.9860	28.9080	200	Kinemetrics, SSA-12, ±2g

[a] Istanbul Earthquake Early Warning and Rapid Response System stations.
[b] BU-KOERI and ITU stations.
[c] ERI stations.

the three strong-motion networks run by KOERI, ITU and ERI. Moment magnitudes of the selected events were obtained from the catalogue prepared by Kalafat et al. [18]. In addition, a recently occurring event with a magnitude M_w=5.1 recorded by the IERREWS was added (Table 1). In total, we used a dataset of 115 records of 12 earthquakes, including 75 records obtained during the two main- and nine aftershocks of the 1999 Kocaeli and Duzce earthquakes. The key criteria for selecting events were: (a) events of $M_w \leqslant 4.5$, (b) focal depth less than 25 km, (c) availability of at least five stations records for each event (d) within the epicentral distances of less than 100 km. Earthquakes with less than five records, except the one with a magnitude of M_w=7.2, are not included in this analysis. These criteria considerably limited our data, and we had to deal with a small number of events. The detailed information about the earthquakes and the stations are given in Tables 1 and 2, respectively.

All the P wave arrivals were picked manually. Then, we used the peak displacements and velocity amplitudes of the first 3 s of the P waveforms on vertical components. The acceleration signals are integrated to velocities and displacements, which are recursively filtered with a one-way Butterworth high-pass filter with a cut-off frequency of 0.075 Hz for removing the low-frequency drift after the integration process [19].

5. Results and discussion

The relation between τ_c and M_w for the Marmara region was tested in off-line mode, and the following relationship is obtained:

$$\log(\tau_c) = 0.142^* M_w - 0.475 \pm 0.1433 \quad (2)$$

or conversely

$$M_w = 7.042^* \log(\tau_c) + 3.345 \pm 1.009 \quad (3)$$

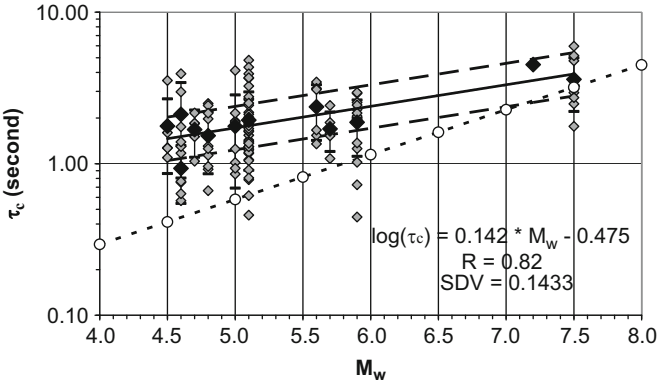

Fig. 3. τ_c and M_w relationship obtained using Kanamori's [2] procedure which is modified from the method used by Nakamura [14]. τ_c estimates with the event-averages and their standard deviations, are plotted for 115 records from 12 events for Marmara Region (gray diamonds). Solid line indicates the least-square fit and two dashed lines show the range of one standard deviation. The dotted line with white circles indicates the linear trend between τ_c and M_w determined from the Japan, Taiwan and southern California records [10].

where τ_c is in seconds. Fig. 3 shows the average τ_c plotted as a function of M_w. The scatter is large, and the average period parameter (τ_c) values, in general, are higher than those determined by other studies (e.g. [4]) especially for small earthquakes. From the early warning point of view, small amplitude data are not of interest. The threshold level for τ_c calculated in this study is about 2 s, and is greater than that calculated for Taiwan (τ_c=1 s), for the events with $M_w > 6$. This may be due to the difference in S/N ratio, especially for smaller earthquakes. Records from the strong-motion networks in Turkey, used in the calculations are mostly 12-bit strong-motion data, and those from Taiwan seismic networks are mainly from 16- or

Please cite this article as: Alcik H, et al. An alternative approach for the Istanbul earthquake early warning system. Soil Dyn Earthquake Eng (2010), doi:10.1016/j.soildyn.2010.03.007

24-bit broadband or strong-motion records. Moreover, the use of strong-motion data involves double integration which occasionally results in long-period drift, and larger τ_c. Fig. 3 also shows a comparison between the $\tau_c - M_w$ relationship derived in this study and that derived by Wu and Kanamori [10].

On the other hand, the noise in the strong motion data at long periods is always a critical issue. Shieh et al. [19] studied this issue by applying different number of poles for the 0.075 Hz high-pass Butterworth filter, one (1) through six (6) poles, and examined the relationship between M_w and τ_c. They pointed out that small number of poles had larger slope but larger scatter. Contrarily, large number of poles resulted in a smaller slope but in a smaller scatter. We used a filter setting with four (4) poles. When compared to other studies, the slope derived in this study is small but less scattered. Although it is an arguable issue, we gave priority to get smaller scattering, thus smaller standard deviation. Moreover, a lower cut-off frequency is more desirable for larger earthquakes, but effect of the long-period noise increases as discussed in [11]. Considering this trade-off, a cut-off frequency at 0.075 Hz was chosen, as is the case in the studies by Wu and Kanamori [11] and by Shieh et al. [19].

On the other hand, Fig. 3 implies that we need at least five stations for a fairly stable estimate of magnitude. With this constraint of current EEW system deployed in the Marmara Region, we need about 10 s to issue a warning signal, depending on the location of a damaging earthquake. The 10 s is the sum of the P-wave travel time to the fifth reporting station, 3 s over which τ_c and Pd are measured, and the delay time of about 1 or 2 s during signal transmission of the current IEEW system. However, warning times could be increased by two approaches. The first one is to use one-station approach like the case in Taiwan [19] and in Japan [11], and the $Pd > 0.5$ cm as an indicator for EEW, which will be discussed later in this part. The second approach could be a dense array in operation. In the case that processing time is less then about 10 s, it will not be possible to issue a warning signal to the sites up to about 30 km from the epicenter, unless we have extended network by at least 10 more stations. This issue is discussed in detail in [23,24]. Figs. 4a and b

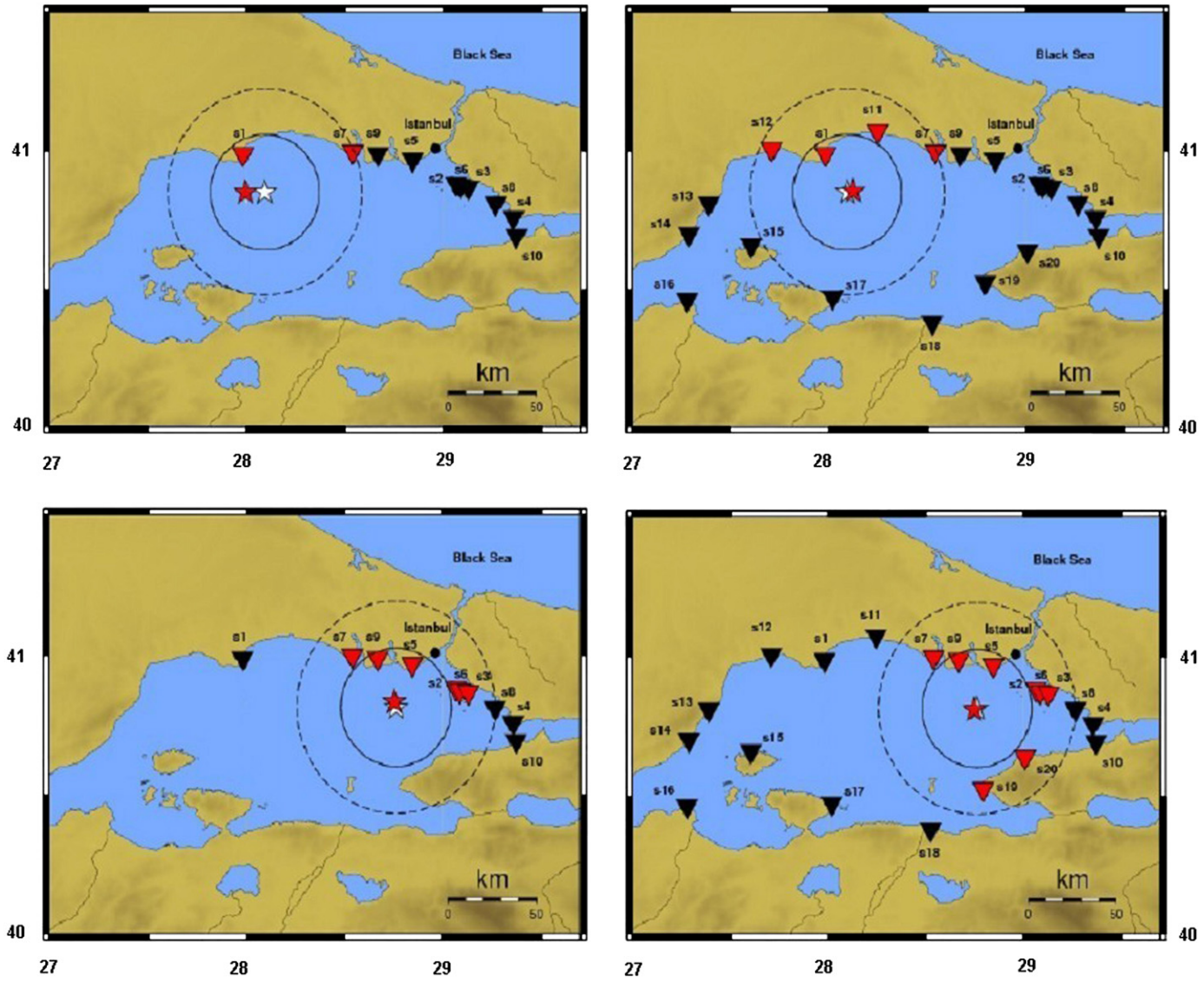

Fig 4. Displayed are the P- (dashed line) and S-wavefronts (solid line) at 0.5, 2.0, 4.0, 8.0 and 15.0 s after the first station was triggered by the P-wave for both the original network of 10 stations (left side) and the extended network (right side). The white star indicates the true epicenter location, whereas the red star is the estimated epicentral location calculated by PRESEIS algorithm, at the given time step. The stations that are already reached by the P-wave are indicated by red inverted triangles, the other ones by black inverted triangles (after [23]). (For interpretation of the references to color in this figure legend, the reader is referred to the web version of this article.)

Please cite this article as: Alcik H, et al. An alternative approach for the Istanbul earthquake early warning system. Soil Dyn Earthquake Eng (2010), doi:10.1016/j.soildyn.2010.03.007

(after [23]) illustrate how an extended network increases warning time. Displayed in these figures are P- and S-wavefronts at 4 s after the first station was triggered by the P-wave for both the current network of 10 stations and the extended network. Apparently, the extended network estimates faster and more accurate whether the occurring earthquake is of potential damage or not. In the frame of the research project, namely Earthquake Disaster Information system for the Marmara region (EDIM, Turkey), the existing early warning network is planned to be extended in the near future to regional scale by installing additional 10 stations around the Sea of Marmara.

As stated above, *Pd* is an important and robust parameter for rapid recognition of damaging earthquakes, since it is more characteristic of the earliest stage of an earthquake's rupture process, and also less affected by the scattering due to the complex velocity structure than the other types of arrivals in estimating magnitudes [10,17,22]. Fig. 5 shows the relationship between *Pd* and *PGV* for the 115 records with the epicentral distances less than 100 km. *PGV* values increase with *Pd* approximately linearly as observed in the other results from Taiwan and Japan [4]. The *PGV*–*Pd* relationship derived in this study is given as

$$\log(PGV) = 0.5654^{*}\log(Pd) + 1.6430 \pm 0.5108 \quad (4)$$

where *PGV* is in centimeters per second and *Pd* is in centimeters. If we take the *Pd* equal to 0.5 cm as a threshold level, the corresponding *PGV* would be about 30 cm/s (Fig. 5), showing that the potential of a damaging earthquake is high. As can be seen in this figure, the damaging earthquakes with M_w=7.2 and 7.5 (Table 1) have the *Pd* values greater than 0.5 cm, and these values belonging to the records from these two events are shown by black-filled circles (Fig. 5).

In the literature (e.g. [9,20]), instrumental intensity scale is given with respect to PGV. Taking the similarity between San Andreas Fault and North Anatolian Fault zone into consideration, and using the relationship between Modified Mercalli Intensity (MMI) and *PGV* (within the range $V <$ MMI $<$ IX) given in [20], the shaking intensity can be estimated as about VII with a standard deviation of 1.5 unit of MMI scale. The large uncertainty is due to the high standard deviation in the *Pd* vs. *PGV* relation. But, on the other hand, Böse et al. [24] set the intensity level as I=5.5 to classify the simulated events into damaging and non-damaging events; all events causing I=5.5 are defined as damaging in the Marmara Region. Thus, the intensity calculated by −one standard deviation is still higher than the intensity level of I=5.5.

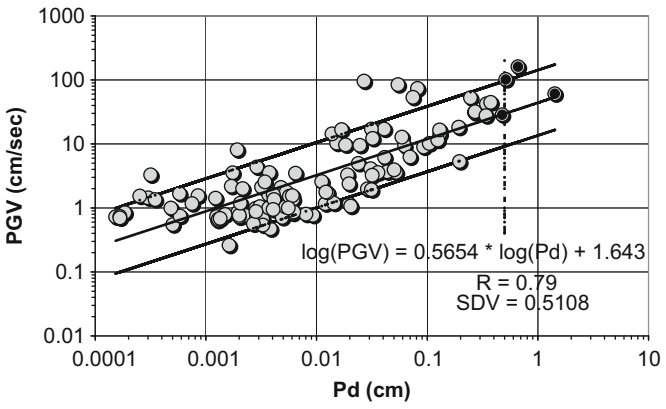

Fig. 5. The relationship between peak–displacement amplitude in the initial 3 s part of the P waves (*Pd*) and PGV for epicentral distances less than 100 km for the Marmara Region. In the process, only vertical components of 115 records from 12 events are used. Solid lines indicate the least-square fit and ±one standard deviation. The black circles indicate the *Pd* values from the records belonging to the two mainshocks (M_w=7.2 and 7.5). Also shown is the threshold level for *Pd* > 0.5 cm.

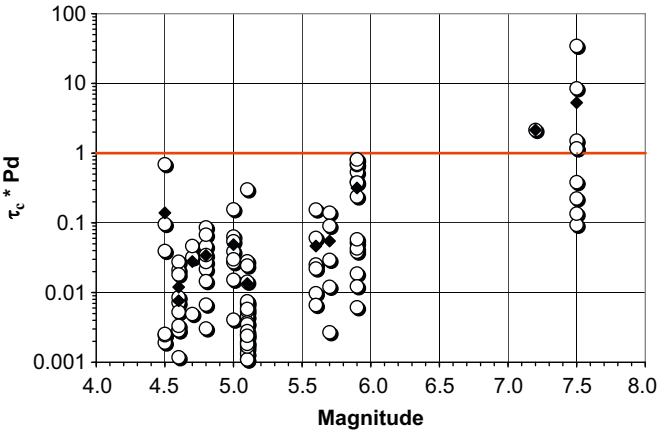

Fig. 6. The relationship between τ_c**Pd* and M_w for the 12 events. Black diamonds show the averages of τ_c**Pd* values for all the records (open circles). The τ_c**Pd* values greater than one belong to the two mainshocks of Izmit and Duzce earthquakes in 1999.

There are 9 records with PGV > 30 cm/s in Fig. 5; four of them have been detected by *Pd* threshold approach (*Pd* > 0.5 cm). On the other hand, five of them are with *Pd* < 0.5 cm. Generally, for a large earthquake with a long rupture length, the *Pd* parameter is measured from the signals produced by the ruptures close to earthquake initials. But, the PGV measurements may be caused by later rupture. Thus, far from the epicenter region, small *Pd* but large PGV [25] may be observed. The epicentral distances of these missed five alerts ranged from 50 to 80 km. However, the regional warning system could offer early warning for such cases.

To improve the reliability and to lessen missed alerts, τ_c and *Pd* can be combined as a single indicator. The product of τ_c**Pd* gives a clearer indicator for discriminating damaging events from non-damaging events. Fig. 6 shows τ_c**Pd* values for all the events used in this study and their averages as a function of M_w. Wu and Kanamori [4] suggested that the product of τ_c**Pd* > 1.0 s cm is a good threshold for identifying damaging earthquakes for Taiwan. When looking at Fig. 6, this threshold level is also consistent with the data from the Marmara Region in Turkey. The two mainshocks with M_w=7.2 and 7.5, which were strongly felt and caused considerable damage, have τ_c**Pd* > 1.0 values. Due to the lack of data in the magnitude range from 6.0 to 7.0, it is not possible to say that τ_c**Pd* values are greater than one or not.

6. Conclusions

The earthquakes of Kocaeli and Duzce in 1999 have initiated the development of a real-time earthquake information system in Istanbul: IERREWS. As part of IERREWS, the IEEWS with an algorithm based on the exceedance of specified threshold time-domain amplitude of PGA and CAV levels, is implemented in 2002. The implemented warning system will provide only warnings regarding the severity of impending strong motion. No information regarding the characteristics of the ground motion is given, and at present, IEEWS is still in progress. The other approaches to earthquake early warning with the use of τ_c and *Pd* methods are explored in off-line mode. As a consequence, empirical relationships both between τ_c and M_w, and between *Pd* and PGV for the Marmara Region are derived and proposed (Figs. 3 and 5, Eqs. (2)–(4)). These two empirical relationships can be used to detect a damaging earthquake within seconds after the arrival of P waves, and can provide on-site warning in the Marmara Region.

Please cite this article as: Alcik H, et al. An alternative approach for the Istanbul earthquake early warning system. Soil Dyn Earthquake Eng (2010), doi:10.1016/j.soildyn.2010.03.007

The reliability can be increased by using the product of τ_c*Pd as a single indicator. As a matter of fact that these relationships are derived by limited data, and therefore, we need to accumulate more data to be able to determine the best threshold values of τ_c and *Pd*. With this limited data, *Pd* appears more effective than τ_c for the Marmara Region, but this issue should also be verified by more data. On the other hand, it is obvious that the best way to assess the robustness and utility of new methods is to implement them on an existing system for real-time testing. Therefore, the relationships determined in this paper can be used to guide the future implementation and progress of the IEEWS in real time after testing for a sufficiently long time.

Acknowledgements

The authors highly appreciate the reviewers for their very constructive suggestions and critics, which helped in improving the manuscript. We also thank the PhD student Miss Berrak Firat for her help in preparing the figures by using GMT software [21]. This work was partially funded by Istanbul University Research Fund under Project number UDP-3564.

References

[1] Erdik M, Fahjan Y, Ozel O, Alcik H, Mert A, Gul M. Istanbul earthquake rapid response and the early warning system. Bull Earthquake Eng 2003;1:157–63.
[2] Kanamori H. Real-time seismology and earthquake damage mitigation. Annu Rev Earth Planet Sci 2005;33:195–214, doi:10.1146/annurev.earth.33.092203.122626.
[3] Wu YM, Kanamori H. Experiment on an onsite early warning method for the Taiwan early warning system. Bull Seismol Soc Am 2005;95:347–53.
[4] Wu YM, Kanamori H. Rapid assessment of damaging potential of earthquakes in Taiwan from the beginning of P waves. Bull Seismol Soc Am 2005;95:1181–5.
[5] Kanamori H, Hauksson E, Heaton T. Real-time seismology and earthquake hazard mitigation. Nature 1997;390:461–4.
[6] Wenzel F, Baur M, Fiedrich F, Ionescu C, Oncescu M. Potential of earthquake early warning system. Nat Hazards 2001;23:407–16.
[7] Nakamura Y. UrEDAS, Urgent Earthquake Detection and Alarm System, now and future. In: 13th world conference on earthquake engineering, Vancouver, BC, Canada, August 1–6, 2004. Paper no. 908.
[8] Espinosa-Aranda JM, Jimenez A, Ibarrola G, Alcantar F, Aguilar A. Mexico City seismic alert system. Seismol Res Lett 1995;66:42–53.
[9] Wu YM, Teng TL, Shin TC, Hsiao NC. Relationship between peak ground acceleration, peak ground velocity, and intensity in Taiwan. Bull Seismol Soc Am 2003;93:386–96.
[10] Wu YM, Kanamori H. Development of an earthquake early warning system using real-time strong motion signals. Sensors 2008;8:1–9.
[11] Wu YM, Kanamori H. Exploring the feasibility of on-site earthquake early warning using close-in records of the 2007 Noto Hanto earthquake. Earth Planets Space 2008;60:155–60.
[12] Erdik M, Demircioglu M, Sesetyan K, Durukal E, Siyahi B. Earthquake hazard in Marmara region, Turkey. Soil Dyn Earthquake Eng 2004;24:605–31.
[13] Alcik H, Ozel O, Apaydin N, Erdik M. A study on warning algorithms for Istanbul earthquake early warning system. Geophys Res Lett 2009;36:L00B05, doi:10.1029/2008GL036659.
[14] Nakamura Y. On the Urgent Earthquake Detection and Alarm System (UrEDAS). In: Proceedings of the ninth world conference on earthquake engineering, vol. 7, 1988. p. 673–8.
[15] Allen RM, Kanamori H. The potential for earthquake early warning in Southern California. Science 2003;300:786–9.
[16] Kanamori H, Maechling P, Hauksson E. Continuous monitoring of ground-motion parameters. Bull Seismol Soc Am 1999;89:311–6.
[17] Wu YM, Kanamori H, Allen RM, Hauksson E. Determination of earthquake early warning parameters, τ_c and *Pd*, for southern California. Geophys J Int 2007;170:711–7.
[18] Kalafat D, Gunes Y, Kara M, Deniz P, Kekovali K, Kuleli HS, et al. A revised and extended earthquake catalogue for Turkey since 1900 ($M \leqslant 4.0$). Istanbul, Turkey: Bogazici University Press; 2007.
[19] Shieh JT, Wu YM, Allen RM. A comparison of τ_c and τ_p^{max} for magnitude estimation in earthquake early warning. Geophys Res Lett 2008;35:L20301, doi:10.1029/2008GL035611.
[20] Wald DJ, Quitoriano V, Heaton TH, Kanamori H, Scrivner CW, Worden CB. Trinet "ShakeMaps": rapid generation of peak ground motion and intensity maps for earthquakes in Southern California. Earthquake Spectra 1999;15:537–55.
[21] Wessel P, Smith WHF. Free software helps map and display data. EOS AGU 1991;72:445–6.
[22] Wu YM, Zhao L. Magnitude estimation using the first three seconds P-wave amplitude in earthquake early warning. Geophys Res Lett 2006;33, L16312, doi:10.1029/2006GL026871.
[23] Köhler N, Wenzel F, Erdik M, Alcik H, Mert A. Earthquake early warning performance tests for Istanbul. Geophysical Research Abstracts, vol. 11, EGU2009-8332, 2009, EGU General Assembly 2009.
[24] Böse M, Wenzel F, Erdik M. PRESEIS: a neural network-based approach to earthquake early warning for finite faults. Bull Seismol Soc Am 2008;98(1):366–82.
[25] Shieh JT, Wu YM, Zhao L, Chao WA, Wu CF. An examination of τ_c–*Pd* earthquake early warning method using a strong-motion building array. Soil Dyn Earthquake Eng, 2009, doi:10.1016/j.soildyn.2009.12.015.

Please cite this article as: Alcik H, et al. An alternative approach for the Istanbul earthquake early warning system. Soil Dyn Earthquake Eng (2010), doi:10.1016/j.soildyn.2010.03.007